Journal of Asian Ceramic Societies xxx (2015) xxx–xxx

HOSTED BY

Contents lists available at ScienceDirect

Journal of Asian Ceramic Societies

journal homepage: www.elsevier.com/locate/jascer

Talc-based cementitious products: Effect of talc calcination

C.J. Ngally Sabouang[a], J.A. Mbey[a,*], F. Hatert[b], D. Njopwouo[a]

[a] University of Yaoundé I, Department of Inorganic Chemistry, Laboratory of Applied Inorganic Chemistry, PO Box 812, Yaoundé, Cameroon
[b] Université de Liège, Département de géologie, Laboratoire de Minéralogie et de cristallochimie, B18, Allée du 6 Août, B-4000 Liège, Belgium

ARTICLE INFO

Article history:
Received 21 May 2015
Received in revised form 4 July 2015
Accepted 13 July 2015
Available online xxx

Keywords:
Talc
Calcination
Enstatite
Struvite
Cement
Compressive strength

ABSTRACT

This study reports the use of calcined talc for cementitious products making. The calcination is used to enhance the availability of magnesium from talc to react with phosphate for cement phase formation. It is shown that previous calcination of talc leads to products having enhanced mechanical performance due to the formation of more cement phase than in products based on raw talc. Talc fired at 900 °C was found to be the one in which magnesium release was maximal. Firing at temperature higher than 900 °C leads to the stabilization of enstatite, which decreased the magnesium availability. The cement phase is struvite, which was better detected on the X-ray patterns of the products involving fired talc. All the products have very rapid setting time and low shrinkage.

1. Introduction

Cements are materials of common use for human welfare. Although these are ancient materials with well-known chemistry, it is necessary to enhance the cement quality and to find new cementitious raw material to overcome the global warming challenge due to the production of the largely used Portland cement. This research area arouses interests, which focuses on the reduction of the CO_2 emission and for alternative cement formulation using non-classical raw materials [1,2]. Indeed, the Portland cements are considered to be a cause of the global warming increase due to the large amount of CO_2 that is produced by the related industries [3]. Another reason to seek for alternative cement formulation is the related energy cost for the production of hydraulic cements [4,5]. In addition, the need of cement products to be used in humid or acidic environments has aroused interest in studies that focused on the development of cements with low setting time. In this category, magnesium phosphate cements (MPCs) are among promising products [6–9]. MPCs are chemically bonded phosphate ceramics, which were discovered and developed as dental cement in the late 19th century [10]. In these materials, the chemical bonding is formed by a through-solution acid-base reaction between dead burned magnesia and phosphate. In early 1970s, magnesium phosphate cements were investigated as structural materials for usage as fast setting repair material. Recently, a wide range of applications of MPC were developed in civil engineering. These include uses of light magnesium cement foamed material [11], and wastes stabilized and solidified [12,13]. MPCs also exhibit improved characteristics such as low setting time, ability to set and harden at low temperature as −20 °C, high bonding strength, and very good durability including resistance to chemical attack and permeation [14].

In the prospect of developing alternative material source of magnesium, we recently reported the possibility to use talc, which is a hydrated layered magnesium silicate [15]. In this study, evidences that magnesium from the talc structure can be involved in a reaction with phosphate to form cementitious products were demonstrated. However, the products' performance, namely compressive strength, was low and when talc was partially replaced by magnesia (MgO) up to 10%, the performance was increased. This was an indication that the mechanical response of the products could be increased if the magnesium contained in talc is made more available for the reaction process. Thermal treatment of the talc was proposed as a potential way to increase magnesium availability.

In the present study, talc was thermally treated at various temperatures and used for cementitious products formulation with potassium dihydrogenophosphate. Fourier transform infrared spectroscopy (FTIR), X-ray powder diffraction (XRPD), and scanning electron microscopy coupled with energy dispersive X-ray

* Corresponding author. Tel.: +237 699 238 925.
E-mail addresses: cngally@yahoo.fr (C.J. Ngally Sabouang), mbey25@yahoo.fr, jambey@uy1.uninet.cm (J.A. Mbey), fhatert@ulg.ac.be (F. Hatert), dnjop@yahoo.fr (D. Njopwouo).

Peer review under responsibility of The Ceramic Society of Japan and the Korean Ceramic Society.

http://dx.doi.org/10.1016/j.jascer.2015.07.003

spectroscopy (SEM/EDS) were used to analyze the products. Setting time, linear shrinkage, and compressive strength are the mechanical parameters that are evaluated.

2. Materials and methods

A talc from Lamal Pougue in the Boumnyébèl area at about 93 km from Yaoundé (Center region, Cameroon) was used. The area description is presented in Nkoumbou et al. [16]. The raw material, indexed T0804, was manually ground and sieved at 100 μm. The chemical composition of this talc is given in Table 1. The infrared and X-ray diffraction characterizations of the raw talc can be found in Ngally Sabouang et al. [15].

The raw talc is thermally treated using a muffle furnace Carbolite, type CWF 11/5. The temperature rate was set at 5 °C/min and for each firing temperature, the sample is left to soak at the final temperature for 2 h. The heating temperature range was from 400 °C to 1000 °C with an increment of 100 °C between two consecutive heating temperatures. The corresponding fired products are indexed consecutively as T400 up to T1000 prior to infrared spectroscopy and X-ray diffraction analyses.

Analytical burned magnesia from Rhône-Poulenc, sieved at 80 μm, was used at a dosage of 10% in replacement of part of talc as previously established [15]. As described in Ngally Sabouang et al. [15], using X-ray diffraction, the product is mainly made of magnesia with some traces of fortesite and dolomite.

Potassium dihydrogenophosphate was purchased from Alfa Aesar and used as phosphate ingredient.

The cement pastes were prepared as follows:

In an acidic solution of potassium phosphate, a known amount of thermally treated talc and, if needed, MgO are added and thoroughly mixed during 5 min using a M&O mixer. The viscous paste obtained is used for samples molding and for setting time determination. The samples were molded using a cylindrical mold having a diameter of 30 mm and a height of 60 mm. The pastes in the mold are vibrated for 10 min on an electrical vibrating table (M&O, type 202, No. 106) to remove entrapped air bubbles. The samples are covered with a polyethylene bag and left for consolidation. The consolidated samples are kept at the ambient temperature (24–27 °C). During samples consolidation, linear shrinkage is evaluated every 7 days up to 28 days. The 28-day samples are used for compressive strength measurement and for SEM/EDX, XRD and FTIR analyses.

Two series of samples are prepared for each thermally treated talc sample: a sample without addition of MgO and a sample containing 10% MgO. For each formulation, the ratio water/dry matter is 0.2 (in absence of MgO) and 0.4 (in presence of MgO) and the ratio phosphate/talc (or phosphate/talc + MgO) is 0.4. The products' indexations are given in Table 2.

Powder X-ray diffraction patterns were recorded using a Philip Panalytical PW3710 diffractometer equipped with an iron anticathode operating with a Fe Kα radiation (λ = 1.9373 Å) at 40 kV and 30 mA. The diffraction patterns were obtained from 5° to 75° with a step of 0.025°.

Infrared spectra were recorded in transmission mode using a Nicolet Nexus spectrometer. The spectra, recorded from 4000 cm^{-1} to 600 cm^{-1} with a resolution of 1 cm^{-1}, are accumulation of 32 scans.

SEM images are recorded using JEOL JSM-840A and for coupled SEM–EDS analysis, an XL 30 microscope by FEI Company is used. The samples were carbon-coated prior to analysis for coupled SEM–EDS.

Setting time was accessed using a Vicat apparatus according to the EN 196-3 standard.

Measurements of linear shrinkage were done using a Calliper on the hardened mortars aged of 1, 7, 14, or 28 days respectively. Linear shrinkage was calculated using the following equation:

$$R_L = \frac{(L_0 - L) \times 100}{L_0}$$

where L_0 is the initial length of specimens at first days and L is the length of specimens after a given number of days [15].

Compressive strength was determined on 28-day cylindrical samples with 60 mm height using an electro-hydraulic press (M&O, type 11.50, No. 21) with capacity of 60 kN. The samples are submitted to a compressive force at average rate of 3 mm/min until the sample failed according to ASTM C 109 standard test method. The compressive strength was calculated using the following equation:

$$\delta = \frac{F}{A},$$

where F is the failure force and A is the cross-section of the sample.

3. Results and discussion

3.1. Characterization of the fired talc

The XRPD patterns of the various calcined talc samples are presented in Fig. 1. It can be noted that for 400–800 °C, no significant transformation is observed. At 800 °C, a decrease of the d_{002} peak of talc at 9.3 Å is observed and was associated with the dehydroxylation of the talc in accordance with the work by Villiéras [17] in which dehydroxylation was found to be situated between 800 °C and 850 °C. At 900 °C, the decrease of this d_{002} peak is more obvious, confirming the dehydroxylation of talc. At this temperature, the appearance of peaks at 2.85 Å, 3.11 Å, and 2.48 Å associated to enstatite formation is observed. At 1000 °C, the enstatite peaks are better defined. As also reported by Villiéras [17], it is observed that during talc firing between 900 °C and 1000 °C, talc is converted to enstatite. Silica, as a product of dehydroxylation, is not detected given that silica is in amorphous form and will crystallize into cristobalite after 1200 °C.

Table 1
Chemical analysis of major oxide in the used talc.

	SiO_2	Al_2O_3	Fe_2O_3	MnO	MgO	CaO	Na_2O	K_2O	TiO_2	P_2O_5	LOI[a]	Total
T0804	51.71	0.61	6.30	0.09	32.08	0.18	<L.D.	<L.D.[b]	0.01	<L.D.	8.01	98.99

[a] Loss on ignition.
[b] Detection limit.

Table 2
Designation of the various formulations with raw or fired talc.

Firing temperature	Raw	500	700	800	900	1000
Formulation without MgO	TB000	TB500	TB700	TB800	TB900	TB1000
Formulation with 10% MgO	TB001	TB501	TB701	TB801	TB901	TB1001

Please cite this article in press as: C.J. Ngally Sabouang, et al., Talc-based cementitious products: Effect of talc calcination, J. Asian Ceram. Soc. (2015), http://dx.doi.org/10.1016/j.jascer.2015.07.003

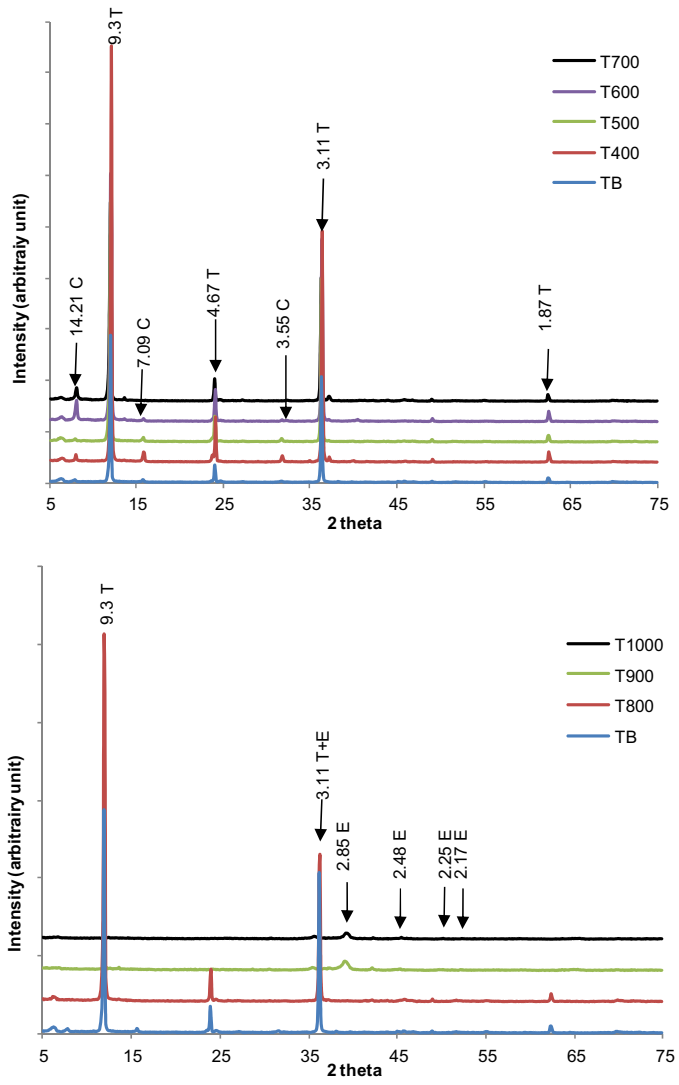

Fig. 1. X-ray patterns of fired talc at various temperatures. TB: raw talc; Tx: fired talc at x °C. T, talc; C, chlorite; E, enstatite.

The infrared spectra of the calcined talc products are shown in Fig. 2. The first obvious modification in the spectra is observable above 800 °C. At 800 °C, the disappearance of the stretching bands of water O—H groups at 3478 cm^{-1}, 3414 cm^{-1} and 3235 cm^{-1} is observed; the stretching band of O—H group in a 2Mg 1Fe environment at 3660 cm^{-1} is reduced and the O—H libration at 669 cm^{-1} is highly decreased due to the dehydroxylation. At 900 °C and 1000 °C, the vibration of O—H disappears and one can clearly observe the vibration bands attributed to the Si—O—Si at 1050 cm^{-1} and 1016 cm^{-1} and the Si—O bands at 938 cm^{-1} and 852 cm^{-1}. These bands evidenced the transformation of talc into enstatite [17]. The disappearance of O—H vibrations bands is an indication of the total conversion of talc into enstatite.

3.2. XRPD and infrared analyses of fired talc-based cementitious products

As found from the analyses of the fired talc products, talc dehydroxylation and conversion into enstatite start at 800 °C. The fired products at 800 °C, 900 °C and 1000 °C were then used for the cementitious products formulation without added MgO. The XRPD patterns of the obtained products are reported in Fig. 3. For these products, all the peaks are characteristic of unreacted

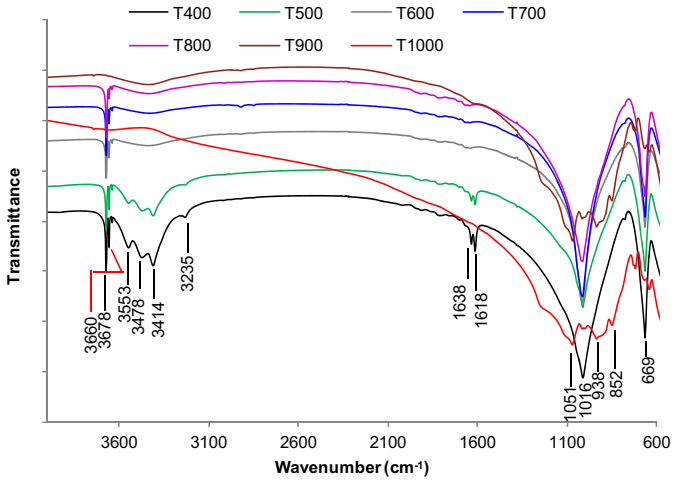

Fig. 2. IR spectra of fired talc at various temperatures. TB: raw talc; Tx: fired talc at x °C.

talc or enstatite. A small hump is observed between 35° and 40° and it is probably due to the formation of an amorphous phase. The unreacted talc, in the product based on talc fired at 800 °C, is evidenced through the peaks at 9.26 Å, 4.70 Å, and 3.11 Å (Fig. 3a). The peaks at 3.70 Å, 3.15 Å, and 2.9 Å are characteristic of the remaining enstatite ($MgSiO_3$) (Fig. 3b). The cementitious phase formed was identified as struvite-K ($MgKPO_4{\cdot}6H_2O$) and the

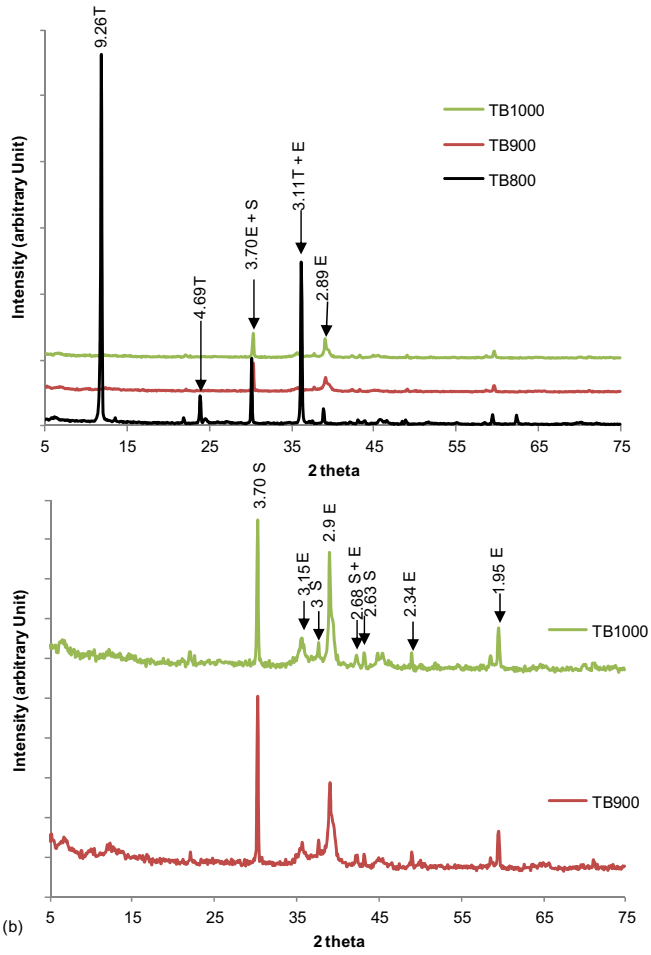

Fig. 3. X-ray patterns of cementitious products based on fired talc at 800 °C, 900 °C and 1000 °C. E, enstatite; S, struvite.

Please cite this article in press as: C.J. Ngally Sabouang, et al., Talc-based cementitious products: Effect of talc calcination, J. Asian Ceram. Soc. (2015), http://dx.doi.org/10.1016/j.jascer.2015.07.003

corresponding diffraction peaks are 3.70 Å, 3.00 Å, 2.68 Å, and 2.63 Å. This phase is formed from the reaction between potassium dihydrogenophosphate and MgO [2]. The relatively large width of these peaks is an indication of poor crystallization of the struvite. It was concluded that there is a coexistence of both crystallized and amorphous struvite. The amorphous form was associated to the hump between 35° and 45° (2 theta unit).

The presence of enstatite in the products is an indication that the MgO in this structure remains poorly reactive. The remaining enatatite and talc acted as filler in the obtained cementitious products.

In Fig. 4, the XRPD patterns of products containing 10% MgO are presented. The presence of struvite-K is noticeable in all the formulations (Fig. 4a and b). Its formation is more marked in product based on fired talc at 900 °C and 1000 °C (Fig. 4b). This observation is in accordance with observations on the previous preparations. At these temperatures (900 °C and 1000 °C), a better evidence for struvite formation was observed. Hence, the increased peaks intensity of struvite is obviously due to reaction of the added MgO. This reactivity induced an increase of cement phase formation, which leads to better mechanical response (Section 3.4). For low firing temperature (400–700 °C), one can note that the struvite formation in the products based on fired talc is more noticeable than in raw talc-based products. This is illustrated in Fig. 4c where the comparison between the cementitious product based on raw talc and the one based on fired talc at 400 °C, clearly evidences struvite peaks (4.24 Å, 3.56 Å, 2.9 Å, and 2.71 Å) in the product based on fired talc at 400 °C. The hypothesis retained is that the elimination of hydration water favors the reaction of the added MgO and even the magnesium contained in the talc.

The FTIR spectra are presented in Figs. 5 and 6. On the spectra without MgO addition (Fig. 5), a band associated to valence vibration of H-bonded water molecules is observed at 3235 cm^{-1}; the band at 1638 cm^{-1} is associated to deformation vibration of water molecules.

The bands between 3700 cm^{-1} and 3400 cm^{-1} are associated to the stretching of OH associated to magnesium (Mg—OH). Specifically, the band at 3678 cm^{-1} is associated to O—H in a 3 magnesium environment (Mg_3—OH) and it is characteristic of talc. The variation of the intensity of these bands indicated that magnesium from

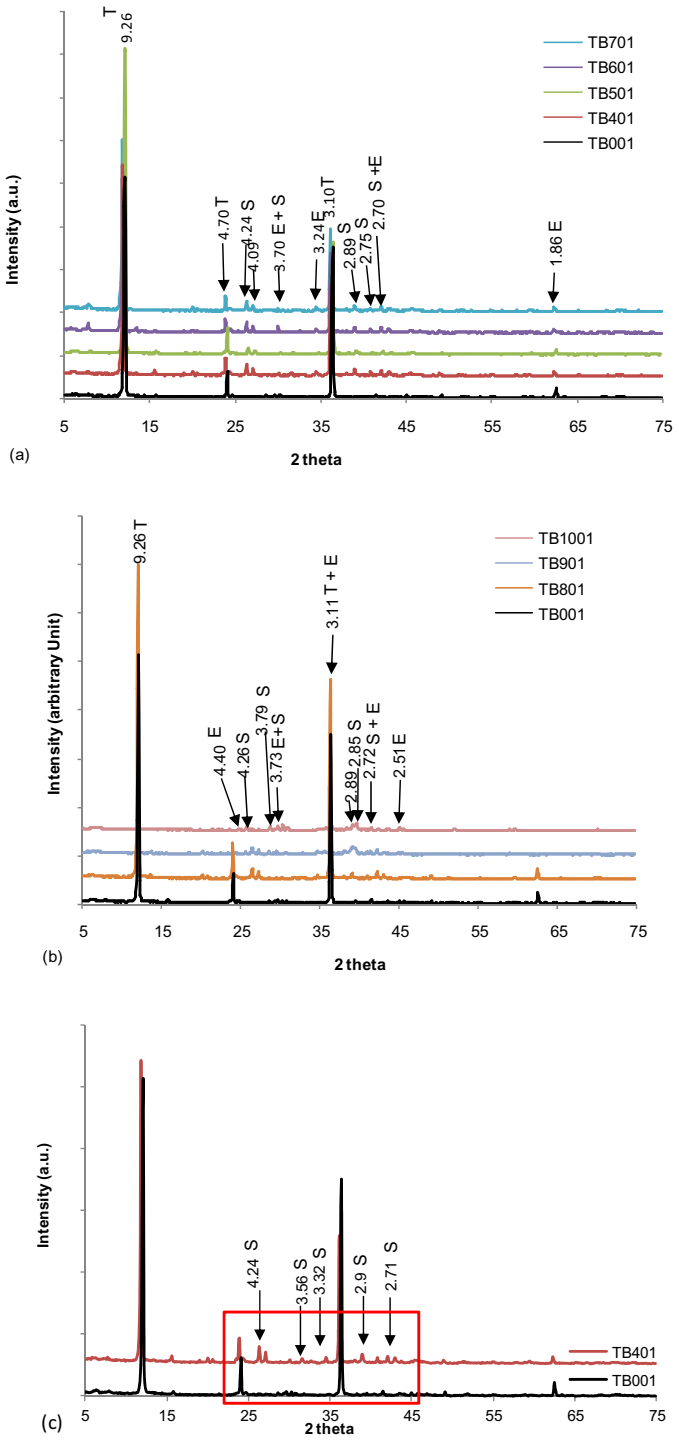

Fig. 4. X-ray patterns of cementitious products based on talc (raw and fired talc at various temperatures) and 10% of MgO. TB001: using raw talc; TBx: using fired talc at x °C. T, talc; S, struvite; E, enstatite.

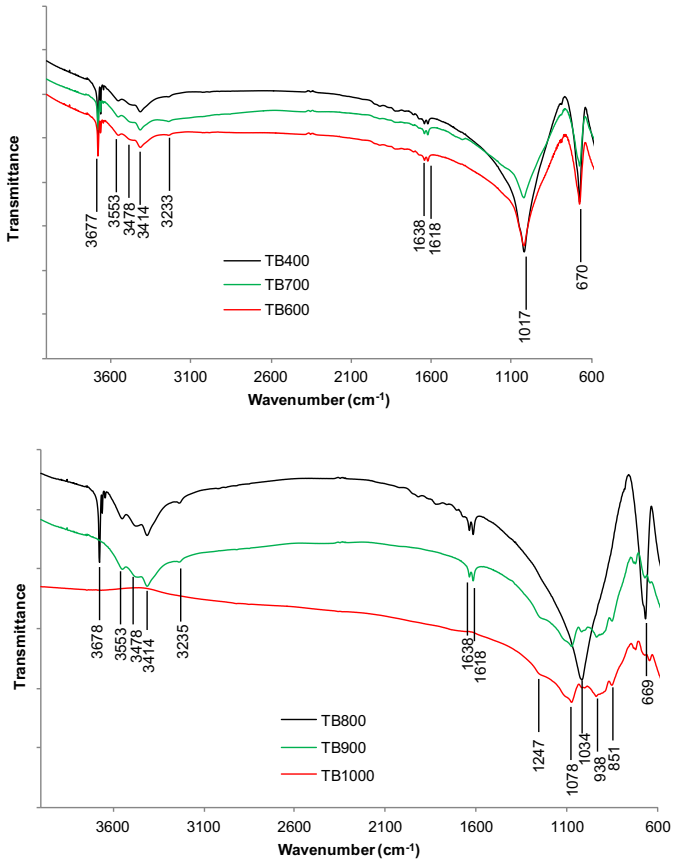

Fig. 5. IR spectra of cementitious products based on fired talc at various temperatures. TBx: using fired talc at x °C.

Please cite this article in press as: C.J. Ngally Sabouang, et al., Talc-based cementitious products: Effect of talc calcination, J. Asian Ceram. Soc. (2015), http://dx.doi.org/10.1016/j.jascer.2015.07.003

talc takes part in the reaction. The libration of OH from the talc is observed at 669–670 cm^{-1}; the decrease of these bands intensities is another indication that magnesium from Mg—OH reacts with the added phosphate.

The asymmetric elongation of Si—O at 1017 cm^{-1} is enlarged due to the superposition to P—O elongation from phosphate. From fired product at 800 °C, bands observed at 1034–1078 cm^{-1} are assigned to antisymmetric elongation of P—O in PO_4^{3-} and the band at 938 cm^{-1} is assigned to P—O—P antisymmetric elongation [18]. The presence of the characteristic bands of phosphate evidenced the presence of phosphate in the matrix of the obtained products.

When 10% MgO is added (Fig. 6), no significant changes are noted on the spectra. The same bands are observable and only an increase in intensity is noted. This increase was associated to the reaction of the added magnesium with phosphate for cement phase formation. From a comparison to previous reported results on raw talc-based cementitious products [15], an increase in cement phase formation upon thermal treatment is deduced. It appears that the thermal treatment increases the reactivity of the magnesium from talc and this is rather more obvious for products based on fired product from 800 °C.

3.3. Linear shrinkage

The results are reported in Fig. 7. It appears that the linear shrinkage is very low (<0.6%) for all the formulations. For all the samples, the maximum shrinkage is achieved after 21 days. The low shrinkage could be due to a good cohesion and low porosity that limit capillary diffusion and hence, shrinkage. In addition, the water dosage in the formulations is favorable for sufficient hydration for cement formation [19,20]. The shrinkage of the products based on fired talc at 800 °C is greater compared to that of other preparations. For the products based on fired talc at 1000 °C, the increased shrinkage is associated to less cement phase formation because of low availability of Mg due to increased stabilization

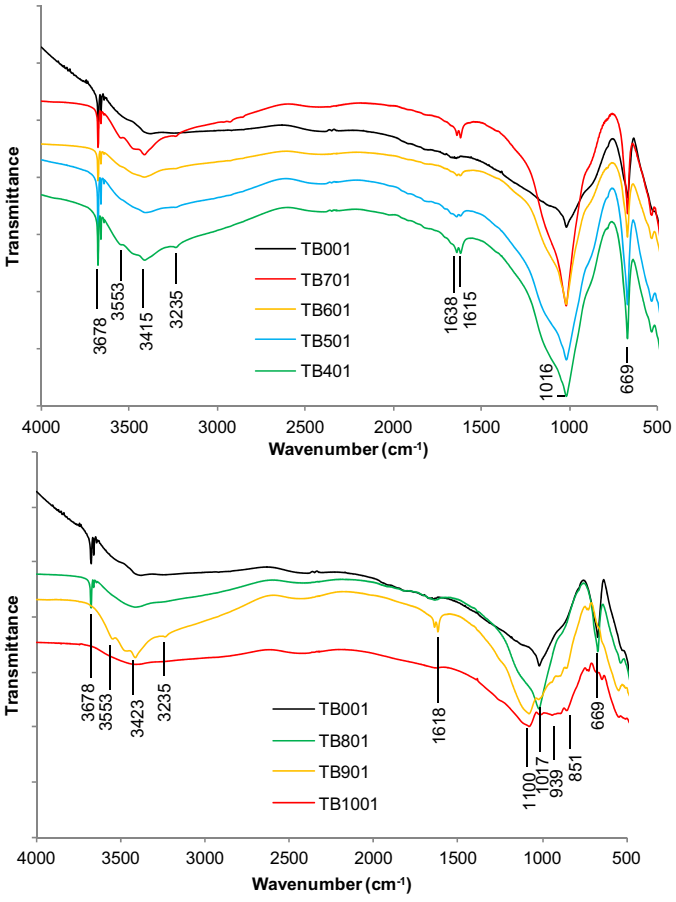

Fig. 6. IR spectra of cementitious products based on talc (raw and fired talc at various temperatures) and 10% of MgO. TB001: using raw talc; TBx: using fired talc at x °C.

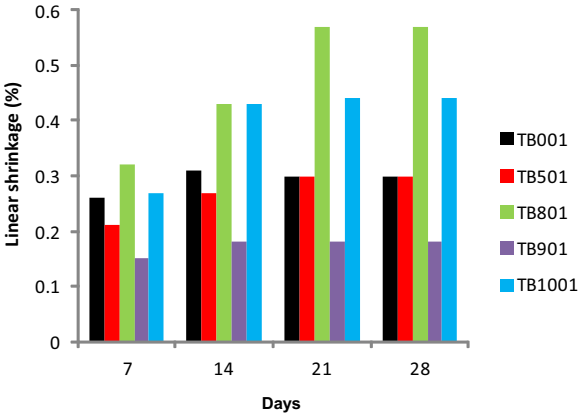

Fig. 7. Linear shrinkage of cementitious products based on 10% MgO and raw or fired talc. TB001: using raw talc; TBx: using fired talc at x °C.

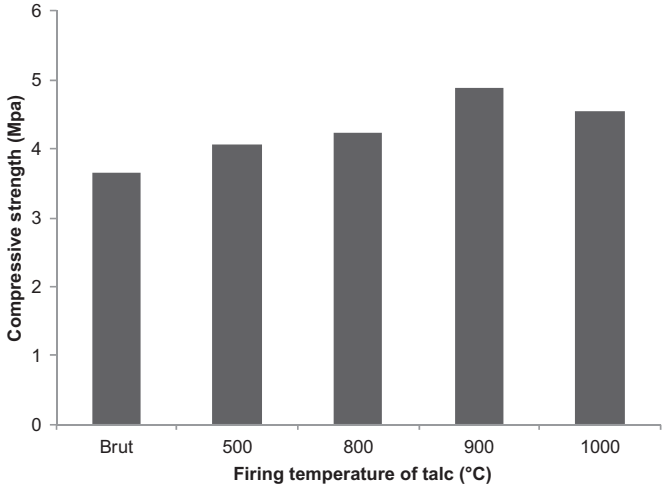

Fig. 8. Compressive strength of cementitious products based on 10% MgO and fired talc.

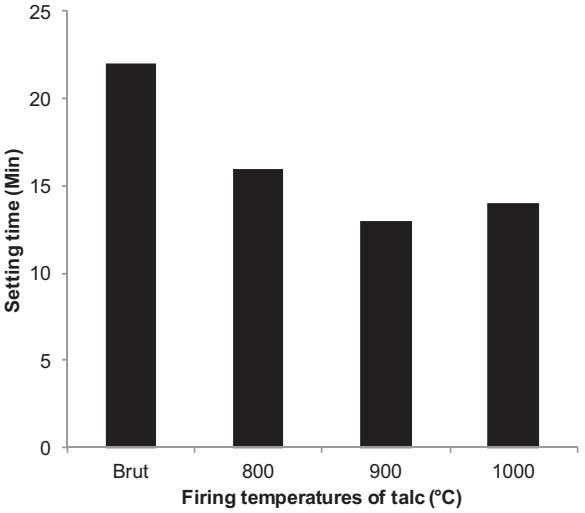

Fig. 9. Setting time of cementitious product with 10% MgO and fired talc.

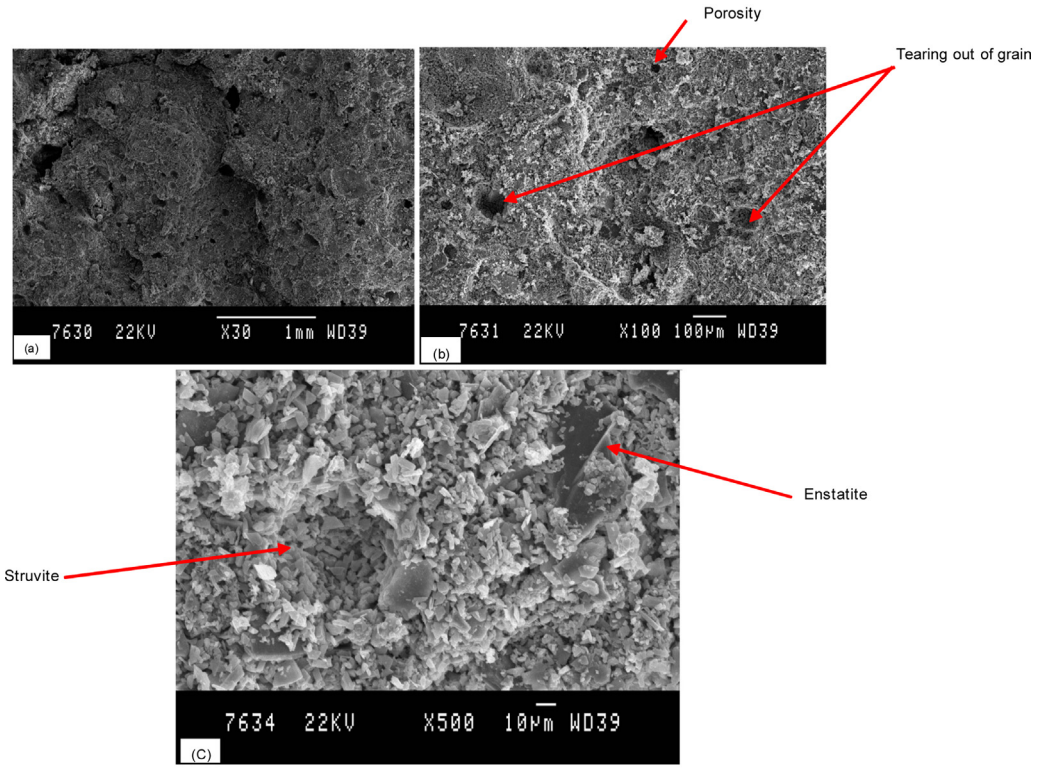

Fig. 10. SEM micrographs of cementitious products based on 10% MgO and fired talc at 1000 °C.

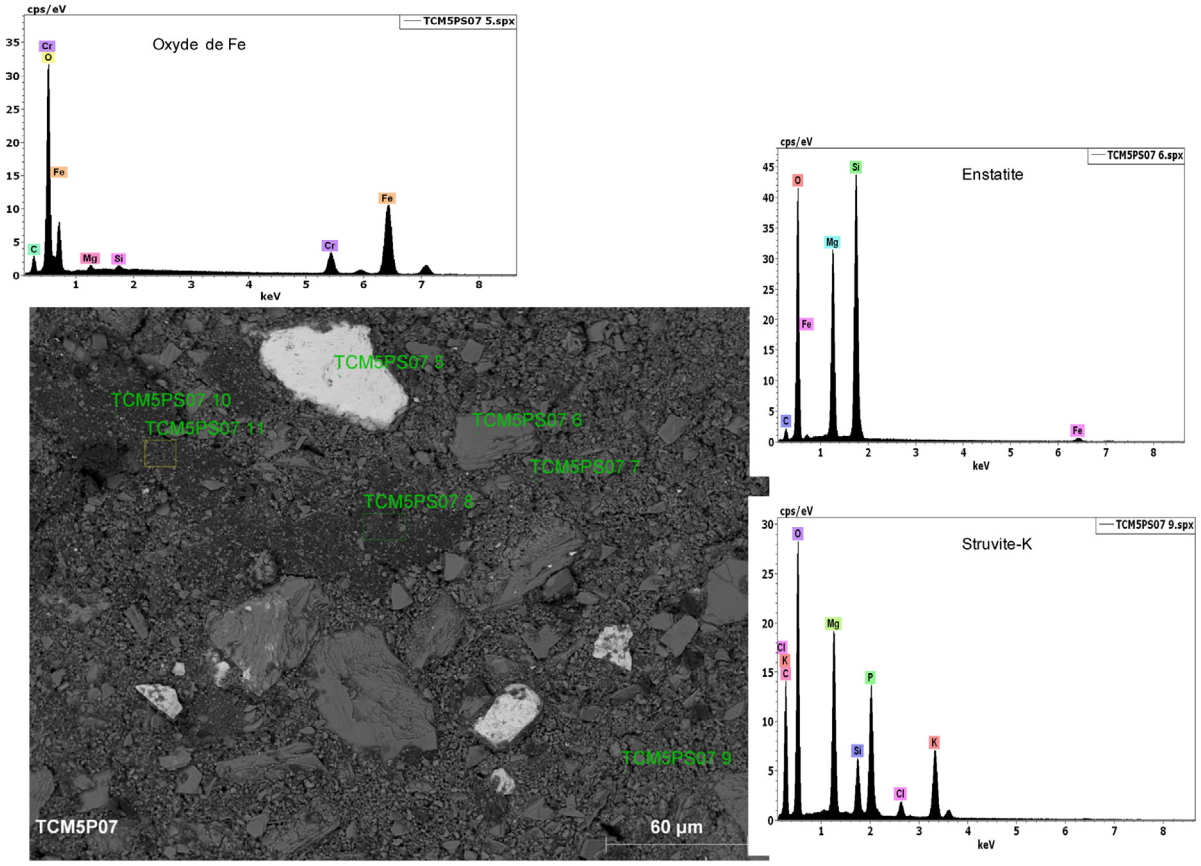

Fig. 11. Coupled SEM–EDS analysis of cementitious products based on 10% MgO and fired talc at 1000 °C.

of the enstatite formed during talc firing. From this conclusion, it was proposed that for the fired talc at 800 °C, the resulting product is composed of a cement phase in which the structure is favorable to shrinkage. A formation of an amorphous cement phase is probably the cause of the observed relatively high shrinkage.

3.4. Compressive strength

The measurements are done on the products with 10% MgO and the results are plotted in Fig. 8. Although the values are low, an increase from 3.66 MPa to 4.88 MPa is observed with increasing firing temperature for talc. At 1000 °C, a decrease is observed in comparison to the product with the talc fired at 900 °C. An increase in cement phase formation, that holds together the particles, accounts for the increase of the mechanical response. Given that the MgO dosage is constant, the differences in the compressive strength are assigned to the availability of the Mg from the fired talc. It is concluded that as the talc firing temperature increases, the availability of reacting Mg for the formation of struvite also increases. At 1000 °C the decrease in compressive strength is associated with an increase of enstatite stability that reduced the Mg availability. For the fired product at 800 °C and 900 °C, the Mg of the enstatite formed is more reactive. As shown by Villiéras [17], the dissolution experiment of enstatite leads to a maximum Mg^{2+} concentration for talc fired at 900 °C. This is in accordance with a maximum availability of Mg from fired talc at 900 °C that leads

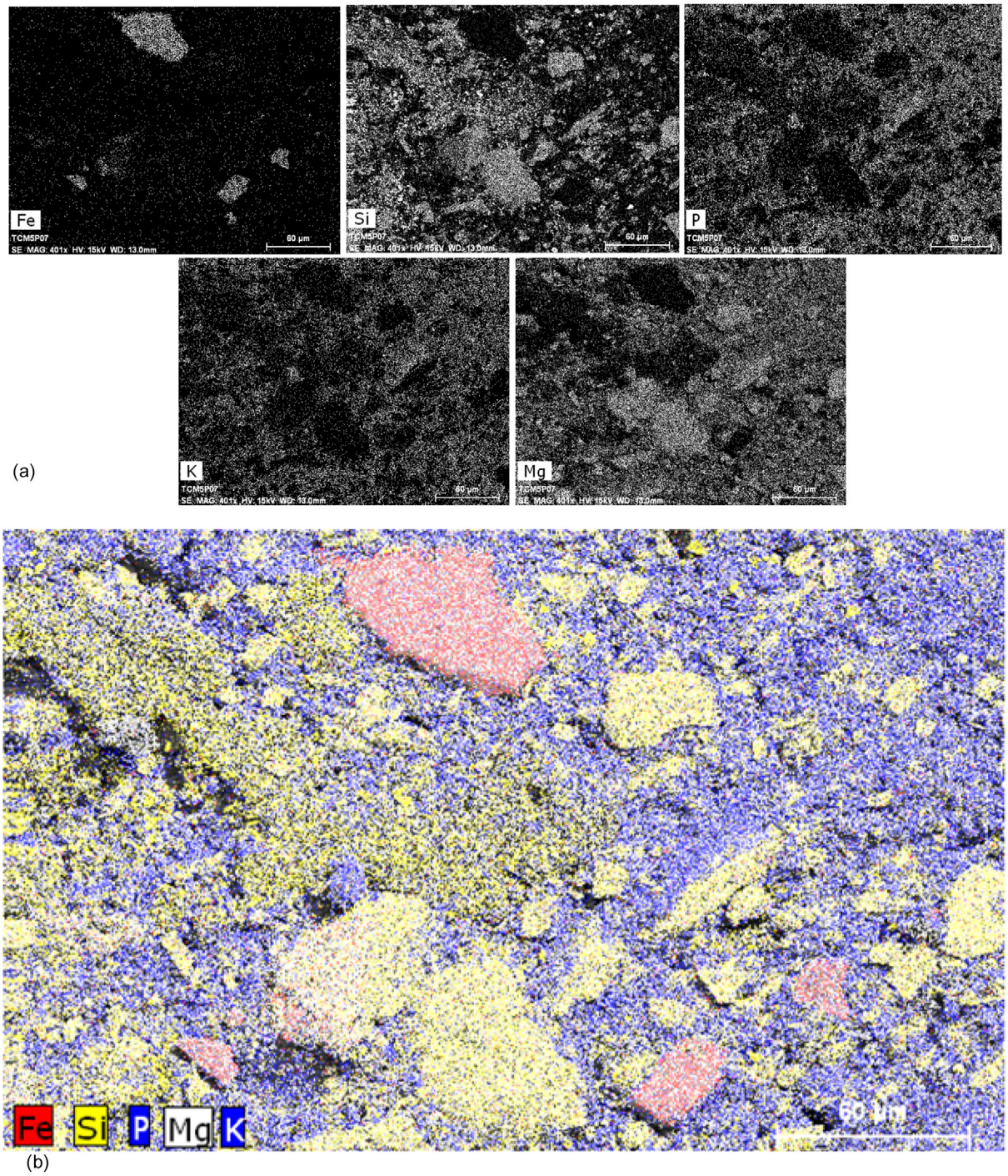

Fig. 12. Elemental map-making on TB1001: (a) for each considered element and (b) reconstitution of the distribution of the various elements analyzed.

Please cite this article in press as: C.J. Ngally Sabouang, et al., Talc-based cementitious products: Effect of talc calcination, J. Asian Ceram. Soc. (2015), http://dx.doi.org/10.1016/j.jascer.2015.07.003

to a cementitious product with maximum value of compressive strength. For the product fired at 500 °C, there is an increase in compressive strength in comparison with raw talc indicating that, even before enstatite formation, Mg in talc is made more available by the dehydration of the talc surface.

3.5. Setting time

The setting time measurements are presented in Fig. 9. These results show a decrease of the setting time from 22 min to 13 min with increasing firing temperature of talc. The setting time is associated to the kinetics of the reaction between the magnesium and the phosphate and depends only on the rate with which the Mg^{2+} ions are made available in the solution given that phosphate dissolution is rapid [21]. The observed reduction of setting time is associated to the crystalline structure of the enstatite formed, which determined the availability of Mg^{2+} ions in the solution. Hence, the lowest setting time registered for the product based on fired talc at 900 °C is justified by the maximum Mg^{2+} in solution that favors the formation of the cement phase (struvite). A small increase of setting time is observed for the formulation with fired talc at 1000 °C and further reinforced the proposal of a more stable enstatite that reduces the Mg availability as proposed from compressive strength.

Given that the product based on raw talc with 10% MgO shows the highest setting time, these results also indicate a better availability of the Mg from talc due to thermal treatment. All the setting times registered are rapid [22].

3.6. Microstructure

The morphological aspect of the cementitious products is presented in Fig. 10. It can be observed in Fig. 10a and b that the structure is homogeneous with holes associated to the tearing out of some remaining enstatite grains, which are imprisoned in the cement matrix. Other holes are attributed to a porosity, which is associated to the organization of struvite grains that composed the cement. In Fig. 10c, two types of crystals can be observed. The larger particles are associated to unreacted enstatite and the smaller crystals are associated to struvite-K, which constituted the cement phase.

The elemental analysis using coupled SEM-EDX is reported in Fig. 11. These elemental analyses allow the identification of unreacting iron oxide (TCM5PS07-5 in Fig. 11). Elemental composition associated with enstatite is shown on the analysis point indexed TCM5PS07-6 (Fig. 11); in the same figure, a composition associated to struvite-K is shown at the point indexed TCMPS07-9. The indexed points TCM5PS07-7, TCM5PS07-8, TCM5PS07-10, and TCPM5PS07-11 also have a composition associated to struvite-K.

Elemental map-making was also done using SEM–EDS (Fig. 12). The distribution of Mg and K elements indicates that these elements are distributed in the same zone and this is due to the fact that it is the reaction between MgO and potassium dihydrogenophosphate that leads to struvite-K formation. The phosphorous (P) distribution follows that of Mg and K and this is obviously due to the reaction previously mentioned. Silica (Si) is an indicator of remaining enstatite. The presence of iron is associated to iron oxide that does not take part in the formation of the struvite. All the observations are reinforced by the global distribution map reconstituted in Fig. 12b. In this figure, K, Mg, and P are superimposed because they take part in the reaction of struvite formation. From this map, it is observed that struvite covers the entire surface and this justifies the homogeneous feature observed on SEM micrographs (Fig. 11). The struvite distribution ensured the imprisoning of remaining enstatite and iron oxide leading to a good cohesion of the products.

4. Conclusion

The aim of this study was to evaluate the influence of the thermal treatment on the availability of Mg from talc in cementitious products preparation. The structural evolution of the talc upon firing indicates that under thermal treatment, talc is converted into enstatite from 800 °C and this conversion is maximal at 900 °C. The formulation of cementitious products using fired talc from 400 °C to 1000 °C shows the following:

1. Even for products without conversion of talc into enstatite, higher compressive strength is obtained in comparison to raw talc. It was concluded that the elimination of surface adsorbed water onto talc favors the availability of Mg from talc to react with the phosphate.
2. When talc is converted into enstatite, the availability of Mg is increased leading to increased cement phase formation with improved mechanical response of the products. Maximum availability of Mg is achieved for fired talc at 900 °C. Firing above 900 °C is not of interest. The enstatite stabilization upon firing above 900 °C did not favor the availability of Mg^{2+} for reaction with the phosphate.
3. The cement phase was found to be struvite-K as evidenced by XRD, FTIR and SEM–EDS analyses. The elemental distribution of Mg, K, and P using coupled SEM–EDS indicates that the struvite covers all the entire surface and ensures the cohesion of the products that favors the improvement of the mechanical responses.

Acknowledgements

The Ministry of Higher Education of Cameroon is greatly acknowledged for a travel grant to Mr. Ngally Sabouang for a research stay at the University of Liège (Belgium).

The University of Liège (Belgium) is acknowledged for analytical facilities to Ngally Sabouang during his stay at Liège (Belgium).

References

[1] D.C. MacLaren and M.A. White, J. Chem. Educ., 80, 623–635 (2003).
[2] E. Soudée, Liants phosphomagnesiens: mécanisme de prise et durabilité (Thèse d'état), Université de Lyon (1999).
[3] J. Davidovits, J. Therm. Anal. Calorim., 37, 1633–1656 (1991).
[4] T. Finch and J.H. Sharp, J. Mater. Sci., 24, 4379–4386 (1989).
[5] D. Singh, A.S. Wagh, J.C. Cunnane and J.L. Mayberry, J. Environ. Sci. Health Part A, 32, 527–541 (1997).
[6] S.S. Seehra, S. Gupta and S. Kumar, Cem. Concr. Res., 23, 254–266 (1993).
[7] A.K. Sarkar, Ceram. Bull., 69, 234–238 (1990).
[8] S. Popovics, N. Rajendran and M. Penko, ACI Mater. J., 84, (1) 64–73 (1987).
[9] Q. Yang, B. Zhu and X. Wu, Mater. Struct., 33, (4) 229–234 (2000).
[10] S. Fan and B. Chen, Constr. Build. Mater., 65, 480–486 (2014).
[11] J. Yunsong, Mater. Lett., 56, 353–356 (2002).
[12] J. Torras, I. Buj, M. Rovira and J. de Pablo, J. Hazard. Mater., 186, 1954–1960 (2011).
[13] S. Iyengar and A. Al-Tabbaa, GeoCongress, 716–723 (2008).
[14] Y. Li and B. Chen, Constr. Build. Mater., 47, 977–983 (2013).
[15] C.J. Ngally Sabouang, J.A. Mbey, Liboum, F. Thomas and D. Njopwouo, J. Asian Ceram. Soc., 2, 264–267 (2014).
[16] C. Nkoumbou, F. Villieras, D. Njopwouo, C. Yonta Ngoune, O. Barres, M. Pelletier, A. Razafitianamaharavo and J. Yvon, Appl. Clay Sci., 41, 113–132 (2008).
[17] F. Villiéras, Etude des modifications des propriétés du talc et de la chlorite par traitement thermique (Thèse nouveau doctorat), Institut national polytechnique de Lorraine (INPL) (1993), 570 pp.
[18] R. Essehli, B. El Bali, S. Benmokhtar, H. Fuess, I. Svoboda and S. Obbade, J. Alloys Compd., 493, 654–660 (2010).
[19] A. Sathonsaowaphak, P. Chindaprasirt and K. Pimraksa, J. Hazard. Mater., 168, 44–50 (2009).
[20] M. Petri and I. Odler, Mater. Res. Soc. Symp. Proc., 179, 83–86 (1991).
[21] J.H. Sharp and H.D. Winbow, in Cements Research Progress, Ed. by W.E. Brown, American Ceramic Society, Westerville, OH (1989) pp. 233–264.
[22] S. Popovics and N. Rajendran, Transp. Res. Rec., 1110, 34–45 (1987).

Please cite this article in press as: C.J. Ngally Sabouang, et al., Talc-based cementitious products: Effect of talc calcination, J. Asian Ceram. Soc. (2015), http://dx.doi.org/10.1016/j.jascer.2015.07.003